Observation of flow structure past a full-stage axial air turbine at the nominal and off-design states

Cite as: AIP Conference Proceedings **2323**, 030004 (2021); https://doi.org/10.1063/5.0041491
Published Online: 08 March 2021

Daniel Duda, Tomáš Jelínek, Martin Němec, Václav Uruba, Vitalii Yanovych, and Pavel Žitek

Observation of Flow Structure Past a Full-Stage Axial Air Turbine at the Nominal and Off-Design States

Daniel Duda[1, a)], Tomáš Jelínek[2, b)], Martin Němec[2, c)], Václav Uruba[1, 3, d)], Vitalii Yanovych[1, e)] and Pavel Žitek[1, f)]

[1]*University of West Bohemia in Pilsen, Univerzitní 22, Pilsen, Czech Republic.*
[2]*Czech Aerospace Research Centre, Ke Kouli 2, Prague, Czech Republic.*
[3]*Institute of Thermomechanics, Czech Academy of Sciences, Dolejškova 5, Prague, Czech Republic.*

[a)]Corresponding author: dudad@kke.zcu.cz
[b)]jelinek@vzlu.cz
[c)]nemec@vzlu.cz
[d)]uruba@kke.zcu.cz
[e)]yanovichvitaliy@i.ua
[f)]zitek@kke.zcu.cz

Abstract. The air flow inside single-stage test turbine is studied experimentally by Particle Image Velocimetry (PIV). Here we report the measurements results at axial-tangential plane just behind the rotor wheel at middle blade radius. We studied one nominal state and two off-design states. We discuss the applicability of resolution of our PIV system to this flow – we can distinguish the largest vortical structures in the shear layers between blade wake and jet, but the bottom part of the cascade is invisible for us at this moment. Spatial distributions of statistical moments of vorticity show a non-classical behavior at the cross-points of stator and rotor jets. We use our previously published algorithm for calculating spatial energy spectrum and display the turbulent kinetic energy colored by different length-scales of the fluctuations.

INTRODUCTION

Despite the green approach in the energetics industry, the classical steam-powered blade based turbine remains the ground source of electric energy. Additionally, the steam turbines are often forced to work in non-nominal states as they have to stabilize the time-varying outcome of the wind turbines and photovoltaic solar cells. But the blade cascade reaches maximum efficiency at the nominal state, where the fluid gives almost all kinetic energy to the rotor wheel, therefore the velocity profile past the stage is axial only – the tangential component contains kinetic energy, which could be transformed. Under a non-nominal state, the fluid passes the blade cascade not in an ideal direction, therefore the shear layers are wider and stronger resulting into more vortices and higher turbulence. The wind turbines have blades with adaptive angle of attack, but this technology is at the current stage of fine mechanics not applicable to the high-temperature and high-pressure steam turbine [1, 2].

In this short article we report the observation of flow structure past a single-stage experimental turbine under off-design regime. We used the method Particle Image Velocimetry (PIV), which measures instantaneous velocity in entire two-dimensional field of view [3]. We performed the measurement at mid-plane covering the tangential and axial directions.

Experimental Setup

The measurement has been performed inside the single-stage experimental turbine at Czech Aerospace Research Centre. The facility is a part of the closed-loop aerodynamic wind tunnel. A level of pressure in the wind tunnel is

19th Conference on Power System Engineering
AIP Conf. Proc. 2323, 030004-1–030004-7; https://doi.org/10.1063/5.0041491
Published by AIP Publishing. 978-0-7354-4067-8/$30.00

maintained by a system of vacuum pumps and a desired air mass flow rate is then provided by means of a twelve-stage radial compressor driven by a 1.3 MW electric motor. The air temperature and humidity are controlled by inter-stage heat exchangers and a condenser dryer, respectively. The turbine rotational speed is controlled by a hydraulic dynamometer. The facility ensures to independently change a pressure ratio, Reynolds number and the rotational speed of the turbine.

The full-stage geometry represents a typical low-reaction stage with nominal ratio of rotor velocity to inlet velocity $u/c = 0.55$ and nominal isentropic Mach number 0.4. Other parameters of the used stator and rotor wheel are listed in Tab. 1. The presented flow characteristics are measured in the tip plane, thus the characteristics, which vary along blade height, are listed at the tip radius only. The angles in Tab. 1 are measured relatively the axial direction, note that some authors measure them relatively to the tangential direction.

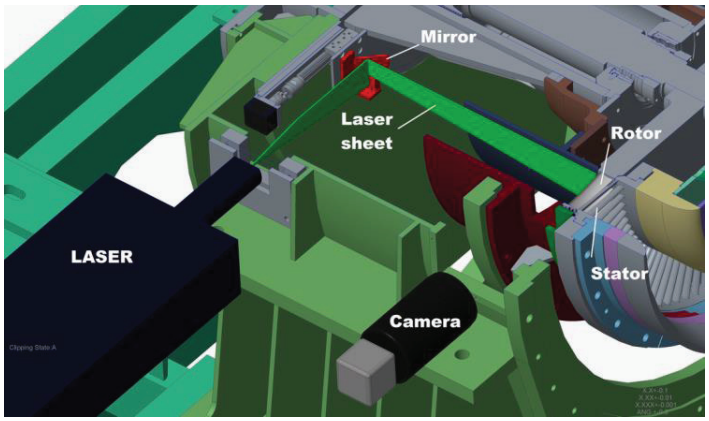

FIGURE 1. Experimental setup (Color version online).

TABLE 1. Parameters of stator and rotor wheel.

Parameter	Unit	Stator	Rotor
Hub diameter	[mm]	440	440
Blade height	[mm]	78.5	80.0
Blade count	[1]	66	82
Designed *u/c*	[1]	0	0.55
Blade pitch (tip)	[mm]	28.42	22.99
Chord (tip)	[mm]	44.61	26.00
t/c (tip)	[1]	0.637	0.884
L/c (tip)	[1]	1.760	3.077
Axial chord(tip)	[mm]	32.62	21.15
Inlet angle (tip)	[°]	0	25
Outlet angle(tip)	[°]	74,5	71,9

An adjustment of the test rig for the PIV setup was done. New optical access in the turbine body was manufactured for the laser, a mirror was placed at the outlet of a diffuser and a window was mounted on the diffuser for the camera access (see Fig. 1). The rotor phase position is measured by using optical gate, whose signal is connected to the PIV system from company Dantec to ensure the synchronization of acquired images with the rotor phase. Our system is the "slow" one, therefore we are not able to measure the time development of individual vertical structures in the flow past rotor. The used lens of focal distance 180 mm together with the camera FlowSense MkII of resolution 2048 × 2048 pixels gives the spatial resolution of acquired images 29.2 × 29.2 mm. The tracer particles are illuminated by solid state double pulse laser New Wave Solo. The time between pulses during this measurement has been 5 μs.

RESULTS

Phase Averaged Velocity Field

Thanks to the phase averaging we can take a look to the mean flow structure as well as to the fluctuations. The stator wheel of this turbine can be rotated slightly in order to investigate the interaction of flow past stator with the flow past rotor.

The flow past rotor wheel overlays the flow structures produced by the stator. As in the case of the near grid turbulence, we can distinguish various regions in this flow system: the *jets* past the interblade channels, the *wakes* past the blades and the shear layers in between. The last ones continuously grow as the turbulence produced here spans into the more homogeneous regions, but at the same time, they become weaker in time with dissipation of smallest vortices.

Figure 2 shows the spatial distribution of output angle of average velocity at nominal and non-nominal state ant at different positions of the stator wheel. The displayed angle α is calculated as

$$\alpha = \arctan\frac{\langle v \rangle}{\langle u \rangle} \tag{1}$$

where $\langle \cdots \rangle$ means ensemble averaging, u and v are the axial and tangential velocity component respectively. We can see alternating strips of larger and smaller angle past the moving rotor blades. The slope of that wakes is, roughly speaking, independent on the actual angle of outcoming flow. These strips are deformed and overlayed by the wake past stator wheel, whose angle reflects the angle of actual velocity (the stator is not moving, the wake is carried). This interaction is not only a passive addition, the lower and higher velocities in the wakes and jets deform the newer flow structures.

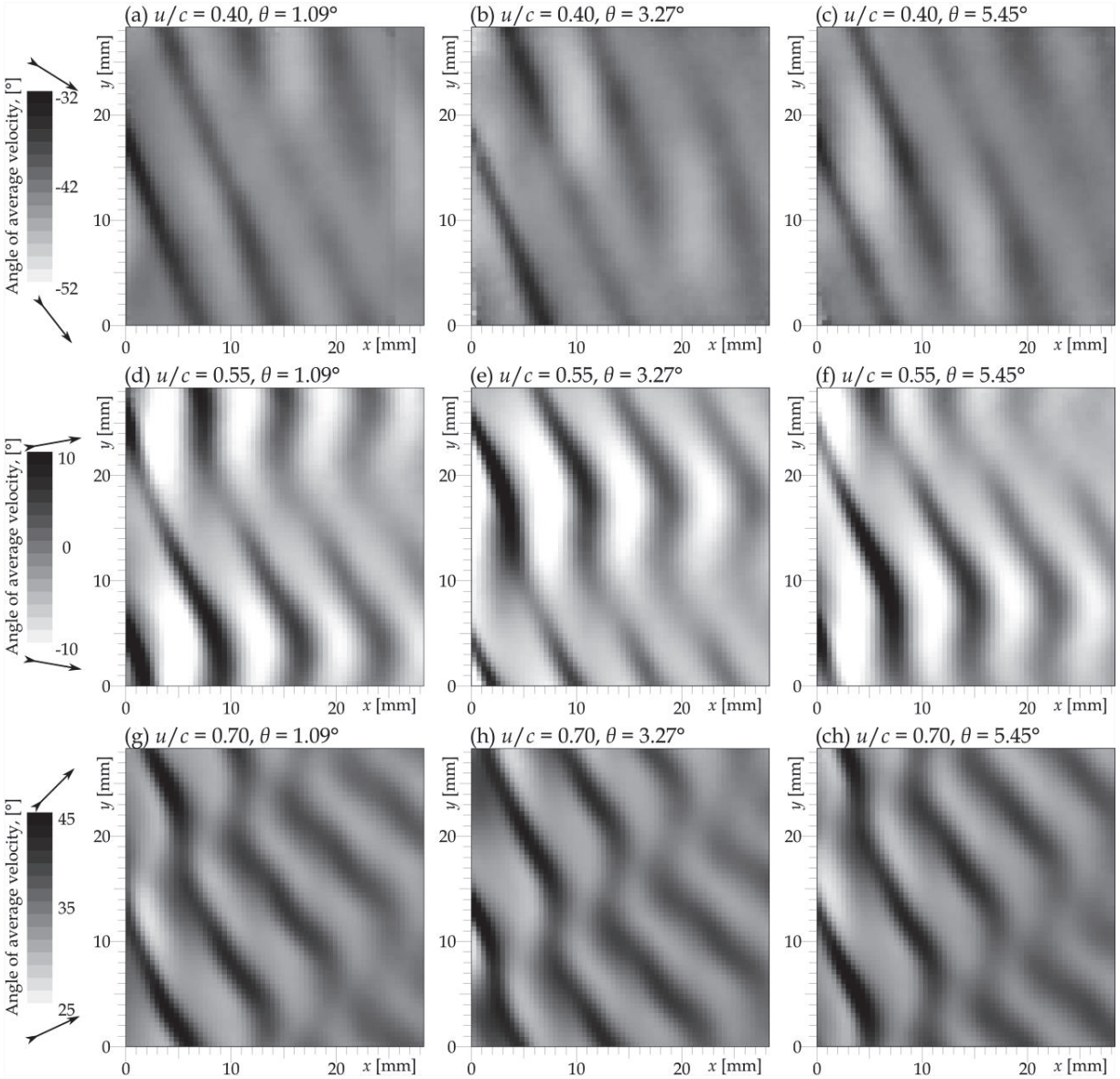

FIGURE 2. Angle of phase averaged velocity field. The panels (a) – (c) show the state with ratio u/c = 0.4. The middle row shows the nominal state u/c = 0.55, the last row (g) – (ch) the state of u/c = 0.7. The columns contain data at different angle θ of stator wheel relative to the measured area such, that the used range of θ covers single distance between blades. The gray-map spans ± 10° around the spatial average of the angle of average velocity and the arrow illustrates corresponding velocity angle. For sake of simplicity, there are not the velocity vectors.

The intensity of turbulence I_T (Fig. 3) is calculated as

$$I_T = 100 \cdot \sqrt{\frac{\langle u^2 \rangle - \langle u \rangle^2 + \langle v^2 \rangle - \langle v \rangle^2}{\langle u \rangle^2 + \langle v \rangle^2}} \tag{2}$$

the fluctuation of the third (radial) velocity component are not included as they are not measured during this 2D-PIV measurement. Thus the real values may differ from the reported ones. The number 100 converts into percentage.

I_T is largest in the nominal state. The wake past rotor blades still contain distinguishable shear layers of little bit higher I_T than the center of the wake.

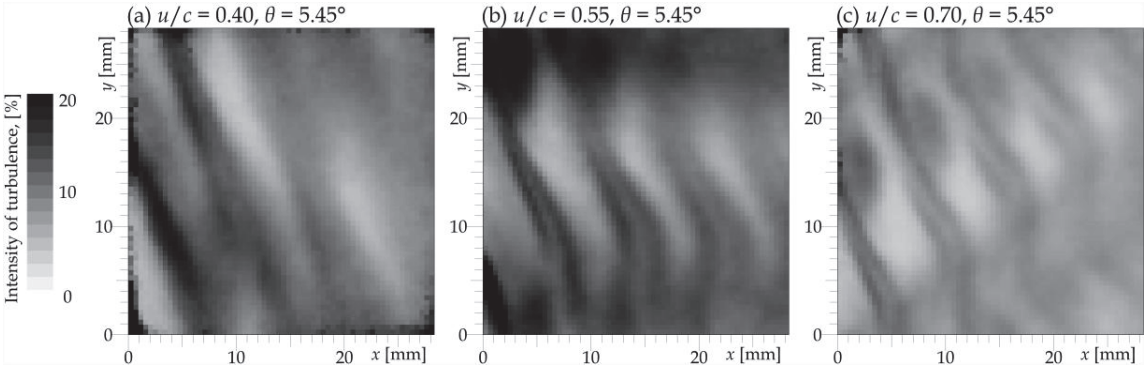

FIGURE 3. Intensity of turbulence at different states at constant stator wheel angle 5.45°. The grayscale is common for all cases from 0 to 20 %.

Instantaneous Vorticity Fields

The vortices grow in the shear layers past the rotor wheel. Their transport is enhanced in the areas of stator wake. Surprisingly, there are not a large difference in the shape of vortices among different rotor wheel velocities. Fig. 4 shows the example of instantaneous vorticities and velocity fields of which is convoluted with the band-pass filter [4] (sometimes called Agrawal decomposition [5]) with σ_D = 0.5 mm and σ_H = 1.8 mm in order to highlight fluctuations of this size interval. The lower bound σ_D of this interval corresponds to a single *Interrogation Area* and it might remove the uncorrelated noise together with real physical structures smaller than that size. The upper bound σ_H removes larger structures [6] such as the entire wakes and jets. The instantaneous vorticity ω displayed in gray-scale in Fig. 4 is calculated as the rotation of instantaneous two-dimensional velocity field

$$\omega = \nabla \times \begin{pmatrix} u \\ v \end{pmatrix} \tag{3}$$

which is calculated on grid with spatial resolution Δx and Δy by using simple symmetrical differential scheme

$$\omega(x,y) = \frac{u(x, y+\Delta y) - u(x, y-\Delta y)}{2\Delta y} - \frac{v(x+\Delta x, y) - v(x-\Delta x, y)}{2\Delta x} \tag{4}$$

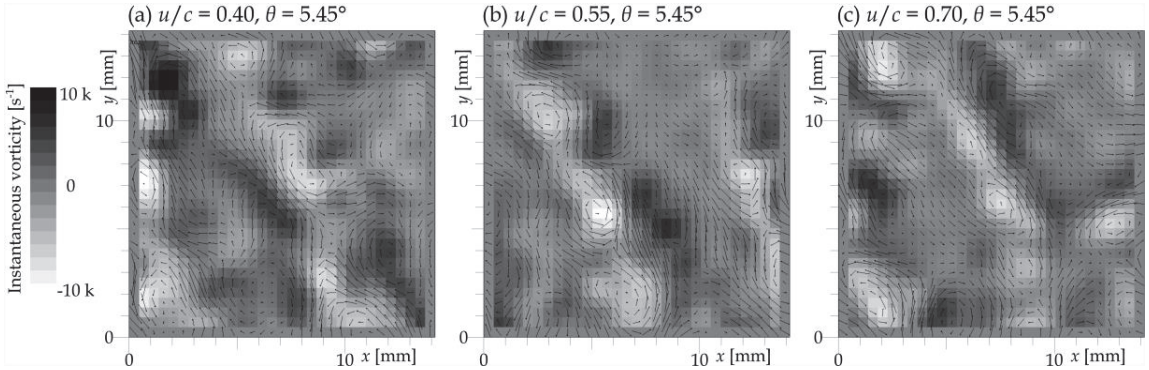

FIGURE 4. Example of instantaneous velocity fields in the central quarter of the field of view. The vectors are convoluted with the band pass filter of size interval 0.5 – 1.8 mm. The grayscale represents the instantaneous in-plane vorticity ω.

The vortices are localized mostly in the shear layers, which is observable in the statistical moments of vorticity. The average of vorticity displays the shear layers, its standard deviation is largest in the area of crossing of wake with jet, as there the vortices are mixed. Contrary, the skewness and flatness display significant deviations inside the cross-point of rotor and stator jets, where the standard deviation of vorticity displays minima (compare panels (b) and (c) of Fig. 5). This deviation in vorticity distribution can be explained via the preferential vortex transport preferring strong vortices of one orientation. This effect weakens as the rotor wake develops.

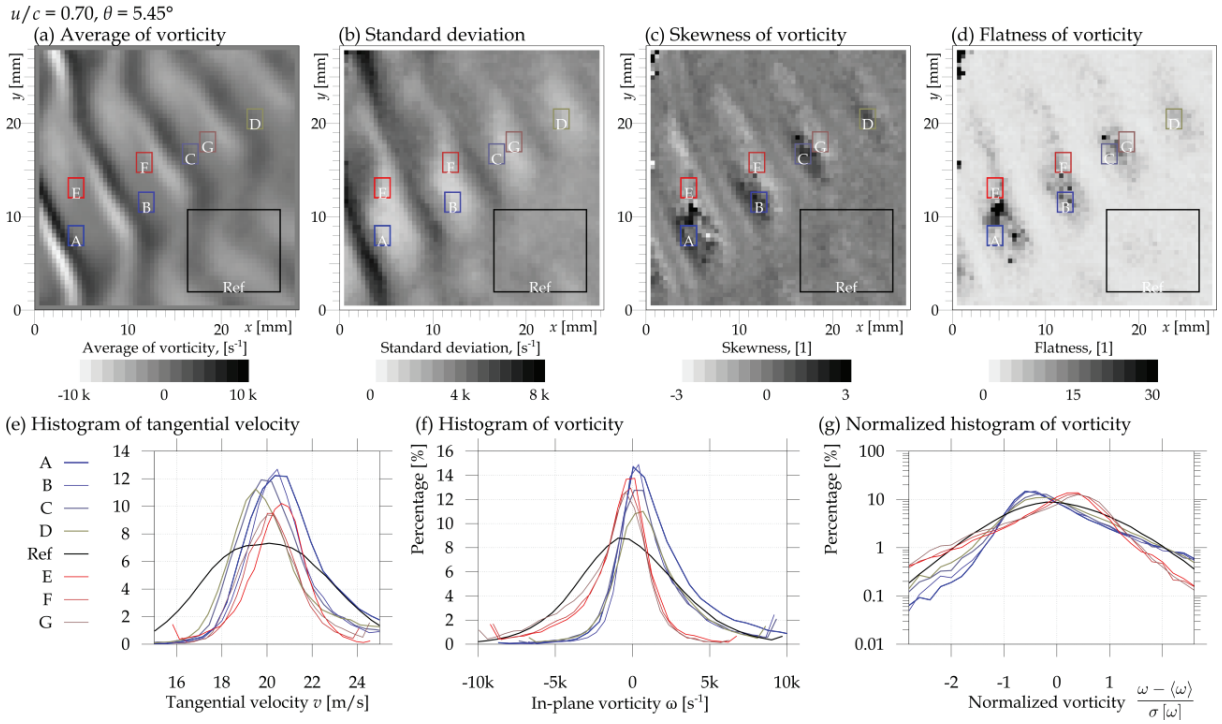

FIGURE 5. Top panels (a – d) show statistical moments of instantaneous vorticity at $u/c = 0.70$. Bottom part (e – f) shows the histograms of tangential velocity (e) and vorticity (f, g) in selected regions denoted A – G together with the reference (Ref) region, where the vorticity statistics displays homogeneous behavior. The regions A – D are selected in the maxima of skewness, E – G in its minima.

Scales of Fluctuations

The autocorrelation function is widely used in flow research [7]. It represents somehow the "memory" of the system, i.e. a statistical connection of events separated by time Δt. Application of Taylor hypothesis allows extension of the correlation into space along streamwise direction. The correlation function in other than streamwise direction refers about the spatial size of typical flow structures passing the reference point. Fig. 6 shows the correlation function of tangential velocity component, which we think to be more relevant for studying the turbulence in this case. The localization of reference point has been chosen in two different possibilities: at the cross-point of rotor wake with the stator wake, where the magnitude of average velocity is minimal (panel (b) of Fig. 6) or the cross-point of jet past rotor wheel with jet past stator wheel, where the magnitude of average velocity is the largest one (panel (c) of Fig. 6).

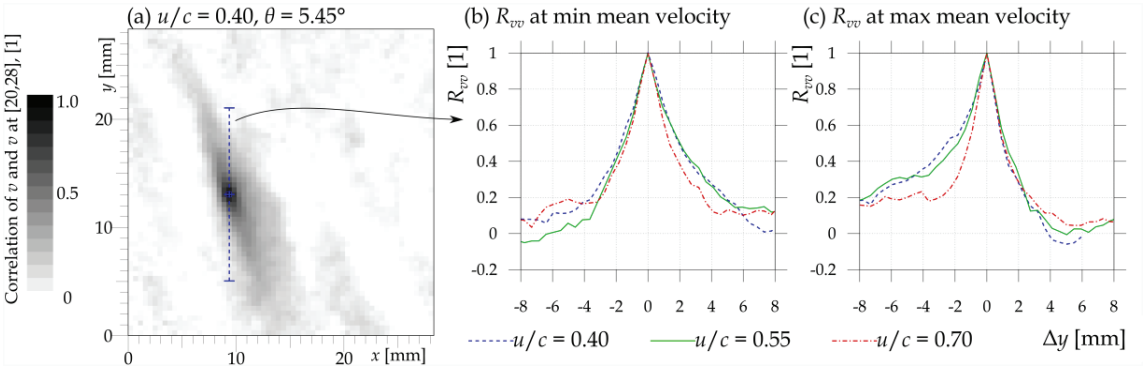

FIGURE 6. The spatial correlation function of tangential fluctuation velocity R_{vv}. Panel (a) shows the spatial distribution of R_{vv} with the point of minimum magnitude of average velocity (a cross of wake with wake) in the state of u/c = 0.40. Panels (b) and (c) show the tangential profile of R_{vv} at different states and in the cross-point of wake with wake (b) and jet with jet (c).

In a classical approach, we can approximate the *Integral length scale* as a distance, where the correlation reaches zero [8]. This approach is quite questionable and strongly depends on what we refer to "reach zero" on a noisy scattered line. In this short report we skip this question and satisfy with the observation of the curves in Fig. 6(b, c) and instead of reaching zero we will discuss reaching 0.2: at the cross-point of wake with wake, it reaches 0.2 around 4 mm in all states. There is an asymmetry between the co-rotor and counter-rotor directions, which is more evident in the correlation with the cross-point of jet with jet. Anyway, the length-scale of largest fluctuations seems to be of order of 4 mm, therefore the used PIV setup is sufficient for recognizing the largest vortices in the wake. On the other hand, the central part of correlation function representing the small vortices is not observable with the current setup.

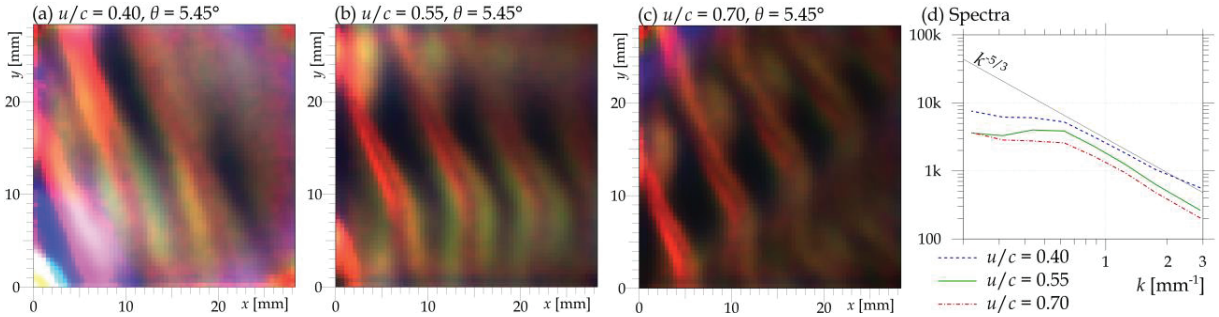

FIGURE 7. The length-scale depending turbulent kinetic energy (TKE). Red colors correspond to TKE of fluctuations of size from 0.5 to 0.7 mm, green colors refer to sizes 1.4 – 1.8 mm and blue color to 3.7 – 5.5 mm. The idea of this plot is to show the information in a three color channels, thus it is impossible to transform it into gray scale suitable for printing. We apologize for this issue. Color version online. Panel (d) shows the spectra of the displayed states, the black line represents the Kolmogorov $k^{-5/3}$ scaling [9, 10].

The length-scale of sources of Turbulent kinetic energy can be determined according to our algorithm described in [6]. It is, roughly speaking, based on the energies of velocity fields of different length-scales obtained by using the band-pass Agrawal filter [4, 5]. The colorful panels of Fig. 7 display the turbulent kinetic energy (TKE) of such velocity fields, when the three perpendicular basic colors (red, green, blue) are used for plotting the spatial distributions of TKE of velocity fields passed through the small, middle and large band-pass filter.

In the current setup, the length-scale dependent fluctuations are dominated by the low-scale term, although some large-scale object can be seen mainly at u/c = 0.40, but, at this moment, we think that this is caused by the noise systematically occurring in the corners of the field of view. The nominal state at u/c = 0.55 nicely shows that the rotor fluctuations widens when passing through the stator wake.

Power spectral density (panel (d) of Fig. 7) roughly follows the Kolmogorov scaling at smaller length-scales (larger wave vectors k) since $k \sim 0.7$ mm^{-1} corresponding to 1.4 mm in direct space. Note the maximum at the nominal state (green solid curve) corresponding to the spatial wave of alternating wakes and jets. In the other states this maximum is not observable in the spectrum, although they contain similar wave as well.

CONCLUSION

We used the experimental method of Particle Image Velocimetry (PIV) for measuring the instantaneous velocity inside the single-stage test turbine located at the Czech Aerospace Research Centre in Prague. This measurement inside this rotating device offers more real insight into the problem than can offer studies of linear blade cascades, which can go into more details, but does not contain a one very important aspect – the rotation. We studied the axial-tangential plane just behind the rotor wheel. Thanks to the synchronization of rotor and PIV system, we distinguish wakes and jets even in the averaged velocity fields. The spatial resolution of our system is reasonable for largest structures in the flow, which has been proven by using the autocorrelation function [7] and by the spatial energy spectrum [6]. The bottom part of the cascade is invisible for us at this moment.

In future we will continue analyzing this data, in focus to the individual vortices and their statistics, we plan to compare this results to some numerical simulation and later we will plan better next measurement learning from the current troubles and inaccuracies.

ACKNOWLEDGMENTS

We thank to Ing. Jan Uher, Ph.D. and Ing Petr Milčák, Ph.D. for inspiration and valuable technical discussions preceding this measurement. We thank to Michaela Vacková for providing transport of equipment and accommodation in Prague.

This work has originated within the framework of the project TN01000007-NCE.

This work was supported by the project of Technology Agency of the Czech Republic TACR No. TH02020057 “Program Epsilon”.

REFERENCES

1. G. Ilieva “A deep insight to secondary flows”, Defect and Diffusion Forum **379**: 83-107 (2017)
2. C. Tropea, A. L. Yarin, and J. F. Foss, “Springer handbook of experimental fluid mechanics”, Springer (2007)
3. D. Jašíková, M. Kotek and V. Kopecký, “An effect of entrance length on development of velocity profile in channel of millimeter dimensions”, AIP Conference Proceedings **1745,** 020018 (2016)
4. A. Agrawal, “Measurement of spectrum with particle image velocimetry”, Experiments in fluids **39** (5): 836-840 (2005)
5. D. Duda and V. Uruba, “PIV of air flow over a step and discussion of fluctuation decompositions”, AIP Conference proceedings **2000**, 020005 (2018)
6. D. Duda and V. Uruba, “Spatial spectrum form Particle Image Velocimetry data”, ASME J of Nuclear Rad Sci. **5** (3): 030912 (2019)
7. E. O. Schulz-DuBois and I. Rehberg, “Structure function in lieu of correlation function”, Applied Physics **24**: 323-329 (1981)
8. R. Azevedoa, L. R. Roja-Solórzano and J. B. Leal, “Turbulent structures, integral length scale and turbulent kinetic energy (TKE) dissipation rate in compound channel flow”, Flow Measurement and Instrumentation **57**: 10-19 (2017)
9. A. N. Kolmogorov, “The Local Structure of Turbulence in Incompressible Viscous Fluid for Very Large Reynolds' Numbers”, Doklady Akademiia Nauk SSSR **30**, 299: 301-305 (1941)
10. S.B. Pope, Turbulent Flows, Cambridge University Press, (2000)